

A Study of Spin Effects on Tennis Ball Aerodynamics

¹FIROZ ALAM, ¹ALEKSANDAR SUBIC, ²JAMAL NASER, ³M.G. RASUL and ³M.M.K. KHAN
¹School of Aerospace, Mechanical and Manufacturing Engineering, RMIT University, AUSTRALIA
²Faculty of Engineering and Industrial Sciences, Swinburne University of Technology, AUSTRALIA
³Faculty of Sciences, Engineering and Health, Central Queensland University, AUSTRALIA
 Corresponding author: firoz.alam@rmit.edu.au

Abstract: Due to complex surface structure, the aerodynamic behaviour of a tennis ball is significantly different compared to other sports balls. This difference is more obvious when spin is involved. Although several studies have been conducted on drag and lift in steady state condition (no spin involved) by the authors and others, little or no studies have been conducted on spin effect. It is known that the spinning can affect aerodynamic drag and lift of a tennis ball thus the motion and flight of the ball. The primary objective of this work was to study the effect of spin using experimental and computational methods. Several new tennis balls were used in experimental study as function of wind speed, seam orientation and spins. A simplified model of a tennis ball was used in computational study using commercial software 'FLUENT'. The simulation results were compared with the experimental findings. The study shows that the spin has significant effects on the drag and lift of a new tennis ball, and the averaged drag coefficient is relatively higher compared to the non- spin condition. The study has also found a significant variation between CFD and EFD results as the complex tennis ball with fuzz elements was difficult to model in CFD.

Key-Words: Drag coefficient, lift coefficient, spin, wind tunnel, EFD, CFD

1 Introduction

The surface structure of a tennis ball is complex due to its fuzzy structure and seam orientation. Hence, the aerodynamics properties of a tennis ball vary significantly from other sports balls. Several studies by Alam *et al.* [1-6], Mehta and Pallis [7-8], Chadwick and Haake [9] described the aerodynamic properties of tennis ball under non-spinning conditions. The aerodynamic behaviour becomes more complex when tennis ball is spun. Apart from the drag and gravitational forces, the lift force is generated due to the spin. The spin affects aerodynamic drag and lift of a tennis ball, and thus the motion and flight of the ball. There is no doubt that the aerodynamics and spin play an important role in the outcomes of sport ball games. Magical tricks by some renowned players such as the short flight (drop) in tennis by Venus William's serve, the curve flight in foot ball by Junior's kick, the curve flight in baseball by Randy Johnson and the flight path in golf by Tiger Wood's drive are well known to many sport lovers. In order to generate a curve flight of a ball through hitting (or serving), throwing and kicking or hitting a ball, the player generally uses the so called Magnus effect. The phenomenon was first observed by German physicist Heinrich Gustav Magnus in 1853. Isaac Newton also described the curved flight of a tennis ball after watching a tennis match. Due to Magnus effect, a spinning ball moving through air produces an aerodynamic force perpendicular to the ball's spin

axis and its cruising direction. This aerodynamic force causes the ball to swing either left or right (depending on clockwise or anti-clockwise spin) if the axis of spin is vertical. If the spin axis is both horizontal and perpendicular to its direction of travel then the ball will either descend faster or slower (due to lift force). When a spinning ball progresses through air, a thin vortex forms, which attempts to rotate at the same speed as the ball. In the region where the vortex rotates toward the oncoming free-stream air, the air close to the surface of the ball decelerates causing the pressure there to increase. Conversely, where the vortex rotates away from the oncoming free-stream air, the air accelerates, causing the pressure there to decrease. The difference in pressures (asymmetric pressure) on the surface of the ball causes the ball to change its direction (deviation or swing). Alam *et al.* [1-5] conducted experimental studies on tennis ball aerodynamics under spinning conditions and found these effects due to spin. The effects of seam and fuzz are believed to be dominant at very low speeds. However, it is generally difficult to measure these effects experimentally at these low speeds since instrumental errors are significant. Additionally, it is generally difficult to measure experimentally the aerodynamic properties of a tennis ball when spin is involved due to mounting complexity on force sensor. A Computational Fluid Dynamics (CFD) method is seen as an alternative tool to the Experimental Fluid Dynamics (EFD) method.

Therefore, the primary objective of this work was to study the aerodynamic properties of tennis balls using CFD method and compare the simulation results with EFD findings. As it is generally difficult to construct fuzz on a tennis ball and mesh the fuzz, a simplified tennis ball model using sphere and spheres with various seam widths was considered in this computational study.

2 Spin Effects on Tennis Ball Aerodynamics

The so called Magnus effect on a sphere due to spin is well known in fluid mechanics. In tennis, apart from the flat serve where there is no or very little spin imparted to the ball, almost all other shots involve some rotation around some axis. As indicated by studies by Alam *et al* [1-6] and Chadwick [10], the lift (or side) force is developed because of Magnus force generated due to the spin. The variation of drag and lift forces and their effects on the motion and flight of the ball due to this spin are of importance and interest.

The focus of this study, therefore, has been on calculating and measuring the lift and drag coefficients (C_L and C_D) in terms of spin parameter.

The aerodynamic drag, lift and side force are directly related to air velocity, cross sectional area of the ball, air density and air viscosity. Drag, lift and side forces are generally defined in fluid mechanics as:

$$D = C_D \frac{1}{2} \rho V^2 A \quad (1)$$

$$L = C_L \frac{1}{2} \rho V^2 A \quad (2)$$

$$S = C_S \frac{1}{2} \rho V^2 A \quad (3)$$

Where C_D , C_L and C_S are the non-dimensional drag, lift and side force coefficients respectively, ρ is the air density (kg/m^3), V is the free stream air velocity (m/s), and A is the cross sectional area of the ball (m^2).

The non-dimensional C_D , C_L and C_S are defined as:

$$C_D = \frac{D}{\frac{1}{2} \rho V^2 A} \quad (4)$$

$$C_L = \frac{L}{\frac{1}{2} \rho V^2 A} \quad (5)$$

$$C_S = \frac{S}{\frac{1}{2} \rho V^2 A} \quad (6)$$

The C_D , C_L , C_S are related to the non-dimensional parameter, Reynolds number (Re) and spin coefficient (α) and defined as:

$$\text{Re} = \frac{\rho V D}{\mu} \quad (7)$$

$$\alpha = \frac{1}{2} \frac{\omega D}{V} \quad (8)$$

Where μ , D and ω are the absolute (dynamic) air viscosity, diameter of the ball and spin rate respectively. Some basic parameters for a range of sports balls are shown in Table 1.

Table 1: Physical dimensions and drag coefficients for various sports balls

Ball types	$\sim C_D$	Diameter (mm)	Mass (g)	Speed m/s	Surface
Foot ball (soccer)	0.5 – 0.2	219.0	427	20	Recess pattern
Golf ball	0.4	42.0	45	70	Recess dimples
Tennis ball	0.6 – 0.65	64.5	57	45	Hairy fuzz
Squash ball	0.4	39.5	24	60	Smooth
Baseball	0.45	70.0	141	40	A seam with over 200 stitches
Cricket ball	0.5	70.0	165	30	Six pairs of seam

3 Experimental Procedure

3.1 Experimental Facilities and Equipment

In order to experimentally measure the aerodynamic properties of a tennis ball, the RMIT Industrial Wind Tunnel was used. The tunnel is a closed return circuit wind-tunnel. The maximum speed of the tunnel is approximately 145 km/h. The rectangular test section dimension is 3 m (wide) x 2 m (high) x 9 m (long) with a turntable to yaw suitably sized objects. A plan view of the tunnel is shown in Fig. 1. The tunnel was calibrated before conducting the experiments and tunnel's air speeds were measured via a modified NPL ellipsoidal head Pitot-static tube (located at the entry of the test section) connected to a MKS Baratron pressure sensor through flexible tubing. Purpose made computer software was used to compute all 6 forces and moments (drag, side, lift forces, yaw, pitch and roll moments) and their non-dimensional coefficients. A mounting device was installed to hold and spin the ball up to 3500 rotation per minute (rpm). The motorised device was mounted on a six component force sensor (type JR-3). Figure 2 shows the experimental set up in the

wind-tunnel test section and the motorised mounting device (right). The distance between the bottom edge of the ball and the tunnel floor was 350 mm, which is well above the tunnel’s boundary layer and considered to be out of ground effect. During the measurement of forces and moments, the tare forces were removed by measuring the forces on the sting in isolation and then removing them from the force of the ball and sting. Since the blockage ratio was extremely low no corrections were made.

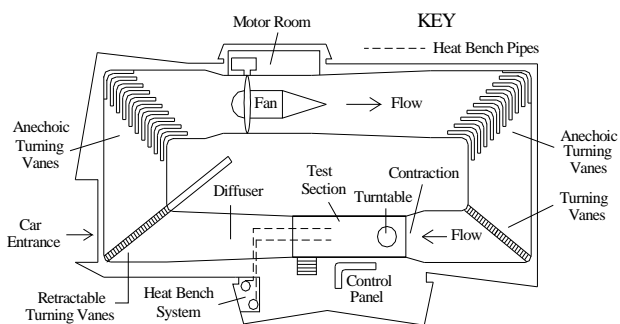


Fig. 1: A Plan View of RMIT Industrial Wind Tunnel (Alam [6])



Fig. 2: A front view of experimental set up in RMIT Industrial Wind tunnel with a motorised supporting device (right)

3.2 Description of Tennis Ball

Several new tennis balls that are officially used in the Australian Open championship have been used for this study. These balls are: Wilson US Open 3, Wilson DC 2, Wilson Rally 2, Slazenger Hydro Guard Ultra Vis 4, Slazenger Hydro Guard Ultra Vis 1, and Bartlett (see Fig. 3). Diameters and masses of these balls are shown in Table 2. The diameter of the ball was determined using an electronic calliper. The width was adjusted so that the ball can slide through the opening of calliper with minimum effort. Diameters were measured across several axes and averaged. As mentioned earlier, these balls were brand new. Fuzz structures of these balls were seen to be slightly different from each other.

Each ball was tested in the wind tunnel under a range of wind speeds (40 km/h to 140 km/h with an increment of 20 km/h) at spin rates of 500, 1000, 1500, 2000, 2500 and 3000 rpm. The ball was spun in relation to vertical axis of the supporting device; hence the side force due to Magnus effect was considered as lift forces.

Table 2: Physical Dimensions of Tennis Balls

Ball Name	Mass, g	Diameter, mm
Bartlett	57	65.0
Wilson Rally 2	57	69.0
Wilson US Open 3	58	64.5
Wilson DC 2	59	64.5
Slazenger 1	57	65.5
Slazenger 4	57	65.5



Fig. 3: Types of Tennis Balls used in experimental study

It may be noted that Wilson Rally 2 ball possesses approximately 8% larger diameter compared to Wilson DC 2 or Wilson US Open 3. This ball was primarily developed to generate larger aerodynamic drag in order to slow the ball speed since presently, top ranking players can introduce ball speed up to 200 km/h. With such high speeds, it is difficult for the viewers to follow the ball’s flight path hence keep interest in the tennis game.

3 Computational Modeling Procedure

In the CFD study, commercial software FLUENT 6.0 was used. In order to understand the simplified model first, a sphere was made using SolidWorks®. Then two simplified tennis ball models without fuzz were also made which are shown in Figures 4 and 5. The simplified tennis balls were constructed with

the following physical geometry: diameter 65 mm, seam with 2 mm width and 1.5 mm depth; and with 5 mm width and 1.5 mm depth respectively. All models were then imported to FLUENT 6.0 and GAMBIT was used to generate mesh and refinement. The major consideration when performing the computational analysis was to perform a simulation with a reasonable amount of computing resources and accuracy. A control volume was created to simulate the wind tunnel and the ball was placed in the control volume. The control volume (wind tunnel) was scaled down to reduce the computational time as the full size wind tunnel was very large compared to the small size of the tennis ball. The sphere was used for a benchmark comparison. The dimensions of the reduced scale wind tunnel are: 2 m long, 1 m wide and 1 m high. As mentioned earlier that a real tennis ball has a textured surface (fuzz) with a convoluted seam (see Fig. 3).



Fig. 4: A 3D sphere CAD model



Fig. 5: A 3D simplified CAD model of tennis ball with 2 mm seam width

In this study only seam effects will be considered as the construction of the filament material (fuzz) of a tennis ball is difficult to construct in CAD and to mesh in CFD. As the accuracy of a CFD solution is primarily governed by the number of cells in a grid, a larger number of cells equates to a better solution. However, an optimal solution can be achieved by using fine mesh at locations where the flow is very sensitive and relatively coarse mesh where airflow has little changes. Tetrahedron mesh with mid-edged nodes was used in this study. Figure 6 shows a model of the tennis ball with the tetrahedron mesh. Generally, the structured (rectangular) mesh is preferable to tetrahedron mesh as it gives more accurate results. However, there are difficulties to use structured mesh in complex geometry. Therefore, in this study, all models were meshed with tetrahedron mesh. The control volume was modeled using GAMBIT. A total of 660,000 hybrid (fine) mesh cells were used for each model. To use fine mesh in the interested areas, sizing function in GAMBIT was used. Mesh validation was done

using Examining Mesh command or “Check Volume Meshes” in GAMBIT. A grid independency test was performed and the 660,000 cells appeared to ensure grid independence. The standard k-epsilon model with enhanced wall treatment was used in CFD computational process. Other model such as k-omega was also used to check any variation in solutions and results.

Velocity inlet boundary conditions were used to define flow velocity at the flow inlet. Flow inlet velocities were from 20 km/h to 140 km/h with an increment of 10 km/h up to 40 km/h and thereafter 20 km/h. However, the data for 40 to 140 km/h was presented in this paper in order to compare with the experimental data. Apart from the calculations using the velocity inlet above, the rotational speed was introduced to define the rotational movement at the ball. The multiple reference frames (MRF) method in rotating coordinate system was used in this study. Outflow boundary conditions were used to model flow exits where the details of the flow velocity and pressure were not known prior to solution of the flow problem. The ball was set to be a wall boundary condition to bound fluid and solid regions.



Fig. 6: 3D CAD model of tennis ball with 5 mm seam width



Fig. 7: CAD model with Tetrahedral mesh

Tangential velocity component in terms of the translational or rotational motion of the wall boundary was specified in order to define the rotational movement of the ball. The introduced rotational speed generates the lift force due to the pressure difference between the top and the bottom side of the ball. In this study, the rotational speeds were: 500 rpm to 4000 rpm with an increment of 500 rpm. The rotational speeds selected were in the same range as used for the experimental measurement. The convergence criterion for continuity equations was set to be 1×10^{-5} (0.001%).

5 Results and Discussion

The results for sphere and simplified tennis balls show similar trends and agree well with the published results. The drag coefficient (C_D) and lift

coefficient (C_L) for the sphere under the range of spin conditions were also computed using CFD which are shown in Figs. 8 and 9 respectively. The drag coefficient and lift coefficient for the simplified model (sphere with seam only-simplified tennis ball with no fuzz) are shown in Figures 9 and 12 respectively. With an increase of spin rate, the drag coefficient increases, however, the drag coefficient reduces as Reynolds number (in wind tunnel experimental study) increases (see Figs. 8 and 9). The trend of reduction of drag coefficients at higher Reynolds numbers is slightly lower compared to that at lower Reynolds numbers. The lift coefficient also increases with the increase of spin rate and decreases with the increase of Reynolds numbers (see Figs. 11 and 12). For higher Reynolds numbers (eg, corresponding to 140 km/h), the reduction of lift coefficients is minimum and the trend of reduction is significantly lower compared to the trend of drag coefficients.

The plots for the experimentally (EFD) found drag and lift coefficients for Wilson Rally 2 tennis ball are shown in Figs. 10 and 13 respectively. In Figure 10, the drag coefficient of a steady condition (no spin involved) is also shown with a thick dark line to compare with the drag coefficients when spin is involved. However, no such line could be shown for lift coefficients since under steady condition no significant lift force coefficient was recorded due to the symmetry of the ball. The drag coefficient for most cases reduces with an increase of speed. The drag coefficients for most cases also increase with spin. However, this increase is minimal at high speeds. At low speeds, the drag coefficients are scattered over a wide range and are volatile. Studies by Alam *et al.* [3, 4] indicated that the drag coefficients at low speeds for steady condition (no spin) are much higher compared to the data at high speeds. Their finding agreed well with Mehta and Pallis [6]. It is generally difficult to measure accurately the aerodynamic forces and moments at low speeds due to the range and sensitivity of the data acquisition. However, for tennis balls, this low speed has a significant influence on the forces and moments as fuzz structures (believed to be very rough at low speeds) play a dominant role in increasing the aerodynamic drag. With an increase of speed, the fuzz orientation becomes more streamlined and reduces the aerodynamic drag. Mehta and Pallis [5] reported that the fuzz can increase the drag of a tennis ball by up to 40% depending on the Reynolds number. The drag coefficient increases with the increase of spin rate at all speeds tested except for the rotational speed of 2000 rpm. It is larger at low speeds but reduces

significantly at high speeds (see Figure 11). It is not clear at this stage why the drag coefficient at this spin rate is relatively higher at low speeds, which is in contrast with other trends. This can be attributed to Reynolds number effect and efforts are being undertaken to investigate this behaviour.

The lift coefficient increases with the increase of spin rates (see Fig. 13). However, the lift coefficient reduces with the increase of wind speeds except the lowest spin (500 rpm). This reduction is more at high rotational speeds (spins). However, the reduction of lift coefficients is minimal at low rotational speeds with the increase of wind speed. The lift coefficient for 2000 rpm spin rate at low wind speeds is relatively higher compared to 2500 rpm spin rate. A similar trend for the drag coefficients was also noted. However, the variation of lift coefficient between 2000 rpm and 2500 rpm becomes minimal at high wind speeds. It is believed that one of the reasons for higher drag coefficients of a tennis ball when spun is due to the characteristics of the fuzz elements. A close visual inspection of each ball after the spin revealed that the fuzz comes outward from the surface and the surface becomes very rough. As a result, it is felt that the fuzz element generates additional drag. However, as the speed increases, the rough surface (fuzz elements) becomes streamlined and reduces the drag. The drag coefficients determined by CFD compared to EFD at low Reynolds numbers are close; however, with the increase of Reynolds numbers, the C_D values are significantly lower. The variation is believed to be due to extreme simplification of the CFD tennis ball (without fuzz). For lift coefficients, a significant variation in magnitudes between the experimental and computational findings is noted. The CFD findings are lower compared to EFD results. However, a similar trend is noted. Again, it is thought to be due to extreme simplification of the CFD tennis ball model.

The CFD results for a sphere and simplified tennis balls indicated no major variation in drag coefficients; however, a significant variation in the magnitude of lift coefficients is noted (see Figures 8-9, 11-12 and Tables 2 and 3). Both drag and lift coefficients exhibit similar trends. The drag coefficients by CFD have some variations compared to the experimental results. The lift coefficient (C_L) found by CFD has significant variations in magnitudes compared to the experimental results. However, both CFD and experimental results have shown similar trends. The variations can mostly be attributed to the omission of surface fuzz in the CFD model. The surface fuzz is not straight forward

surface roughness as it can change with speed and rotation. A sub-critical effect will be required to include it in CFD model. Using the standard approximations formula, approximate error of 1.5% in forces coefficients was found both in experimental and computational studies, which can be considered within acceptable limits.

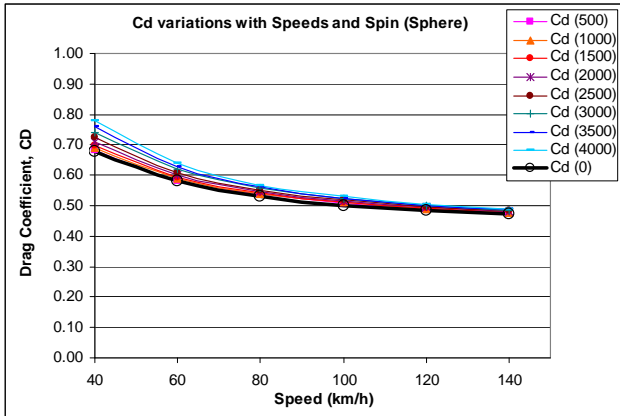


Fig. 8: CFD results: C_D as a function of spin rate and velocity, sphere

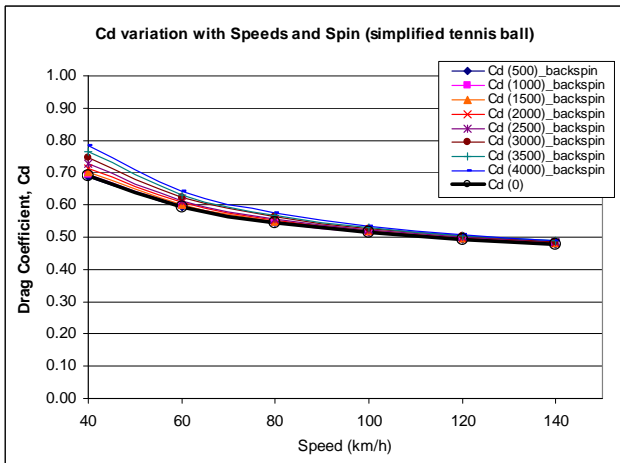


Fig. 9: CFD results: C_D as a function of spin rate and velocity, simplified tennis ball

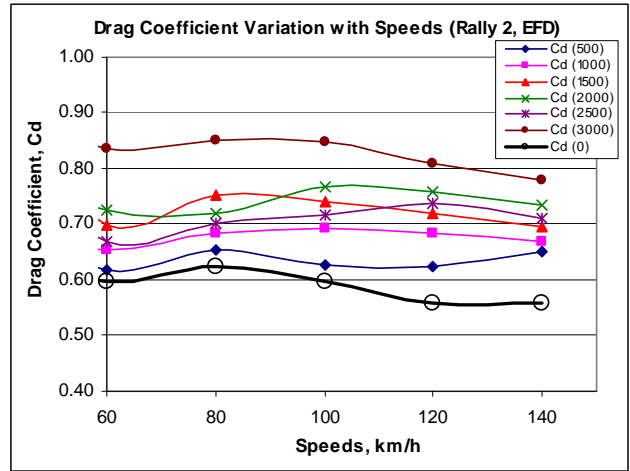


Fig. 10: Experimental results (EFD): C_D as a function of spin rate and velocity, Wilson Rally 2 tennis ball (EFD)

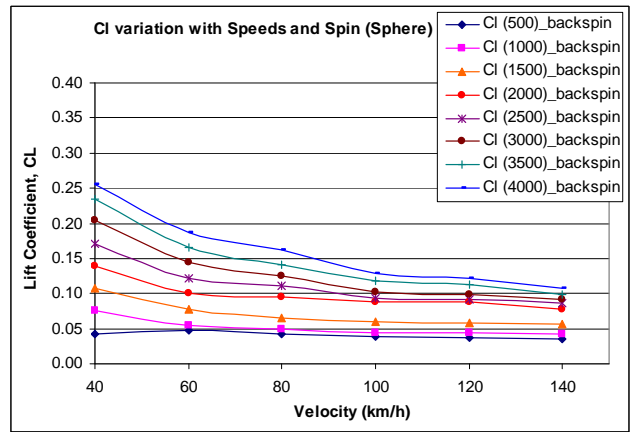


Fig. 11: CFD results: C_L as a function of spin rate and velocity, Sphere

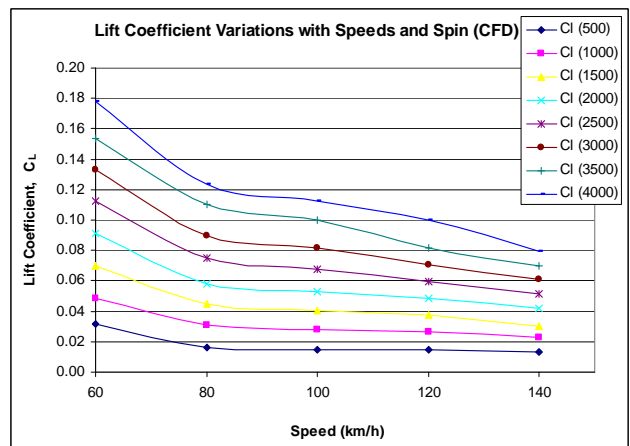


Fig. 12: CFD results: C_L as a function of spin rate and velocity, simplified tennis ball

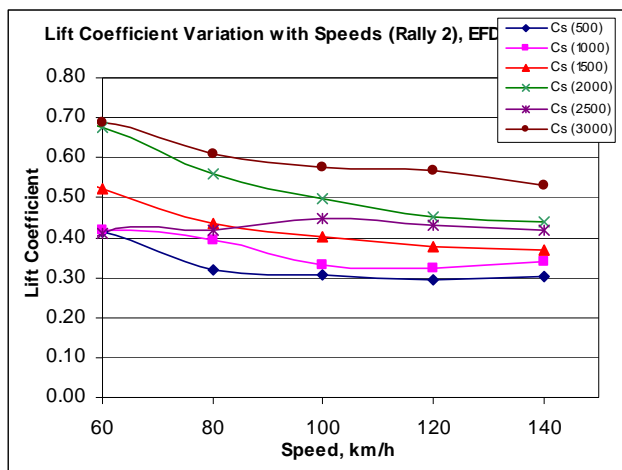


Fig. 13: Experimental results (EFD): C_L as a function of spin rate and velocity, Wilson Rally 2 tennis ball

Table 3: Drag and lift coefficients for a sphere (CFD)

Sphere										
Spin Rate	Backspin		Backspin		Back Spin		Backspin		Backspin	
	60 km/h		80 km/h		100 km/h		120 km/h		140 km/h	
rpm	Cd	Cl	Cd	Cl	Cd	Cl	Cd	Cl	Cd	Cl
500	0.58	0.05	0.54	0.04	0.51	0.04	0.49	0.04	0.47	0.04
1000	0.59	0.05	0.54	0.05	0.51	0.04	0.49	0.04	0.48	0.04
1500	0.59	0.08	0.54	0.06	0.51	0.06	0.49	0.06	0.48	0.06
2000	0.60	0.10	0.55	0.10	0.52	0.09	0.50	0.09	0.48	0.08
2500	0.61	0.12	0.55	0.11	0.52	0.09	0.50	0.09	0.48	0.09
3000	0.62	0.14	0.56	0.13	0.52	0.10	0.50	0.10	0.49	0.09
3500	0.63	0.17	0.56	0.14	0.53	0.12	0.50	0.11	0.49	0.10
4000	0.64	0.19	0.57	0.16	0.53	0.13	0.50	0.12	0.49	0.11

Table 4: C_D and C_L for a simplified tennis ball (CFD)

Simplified Tennis Ball with 5 mm Seam Width										
Spin Rate	Backspin		Backspin		Back Spin		Backspin		Backspin	
	60 km/h		80 km/h		100 km/h		120 km/h		140 km/h	
rpm	Cd	Cl	Cd	Cl	Cd	Cl	Cd	Cl	Cd	Cl
500	0.59	0.06	0.54	0.08	0.51	0.08	0.49	0.08	0.48	0.08
1000	0.60	0.08	0.55	0.13	0.52	0.10	0.50	0.10	0.48	0.10
1500	0.60	0.11	0.55	0.12	0.52	0.12	0.50	0.11	0.48	0.11
2000	0.61	0.15	0.55	0.13	0.52	0.13	0.50	0.12	0.48	0.11
2500	0.61	0.18	0.56	0.13	0.52	0.13	0.50	0.12	0.48	0.12
3000	0.62	0.20	0.56	0.14	0.53	0.13	0.50	0.12	0.49	0.12
3500	0.63	0.25	0.57	0.14	0.53	0.14	0.50	0.13	0.49	0.12
4000	0.64	0.25	0.57	0.15	0.53	0.14	0.51	0.13	0.49	0.13

6 Conclusion

The following conclusions are made from the work presented here:

- The spin has significant effects on the drag and lift of a new tennis ball. The averaged drag coefficient is relatively higher compared to the non-spin condition.
- The lift force coefficient increases with spin rate. However, the increase is minimal at the higher speeds.

- The rotational speed can play a significant role at the lower speeds.
- Spin increases the lift or down force depending on the direction of rotation at all speeds. However, the increase is minimal at high speeds.
- A significant variation between CFD and EFD results was found as the complex tennis ball with fuzz elements is difficult to model in CFD
- Although the CFD results cannot be used for experimental validation, they can be used for quantitative values for drag and lift
- In order to improve the accuracy of CFD results, it is required to model the fuzz element and mesh it correctly

Acknowledgements

The authors express their sincere thanks to Mr Wisconsin Tio, School of Aerospace, Mechanical and Manufacturing Engineering, RMIT University for his assistance with the CFD modelling of simplified tennis balls.

References:

- [1] Alam, F., Tio, W., Subic, A., and Watkins, S., "An experimental and computational study of tennis ball aerodynamics", 3rd Asia Pacific Congress on Sports Technology in The Impact of Technology on Sport II (edited by F. K. Fuss, A. Subic and S. Ujihashi), Taylor & Francis, London, ISBN 978-0-415-45695-1, 2007, pp. 437-442.
- [2] Alam, F., Subic, S. and Watkins, S., "An experimental study of spin effects on tennis ball aerodynamic properties", Proceedings of the 2nd Asia Pacific Congress on Sports Technology, Tokyo, Japan, 12-16 September, 2007, ISBN 0-646-45025-5, pp. 240-245.
- [3] Alam, F., Tio, W., Watkins, S., Subic, A. and Naser, J., "Effects of Spin on Tennis Ball Aerodynamics: An Experimental and Computational Study", Proceedings of the 16th Australasian Fluid Mechanics Conference, ISBN 978-1-864998-94-8, 3-7 December, Gold Coast, Australia, 2007, pp 324-327
- [4] Alam, F., Watkins, S., and Subic, S., "The Aerodynamic Forces on a Series of Tennis Balls, Proceedings of the 15th Australasian Fluid Mechanics Conference, University of Sydney, Australia, 13-17 December, 2004
- [5] Alam, F., Subic, S. and Watkins, S., "Effects of Spin on Aerodynamic Properties of Tennis Balls, Proceedings of the 5th International Conference on Sports Engineering, University

of California, Davis, USA, 13-16 September, 2004, Vol. 1, pp. 83-89.

- [6] Alam, F., "The Effects of Car A-pillar and Windshield Geometry on Local Flow and Noise", PhD Thesis, Department of Mechanical and Manufacturing Engineering, RMIT University, 2000, Melbourne, Australia
- [7] Mehta, R., Alam, F., and Subic, S., "A Review of Tennis Ball Aerodynamics", Sport Technology, Vol. 1, No. 1, February, 2008
- [8] Mehta, R. and Pallis, J. M., "The aerodynamics of a tennis ball", Sports Engineering, Vol. 4, No. 4, 2001, pp. 1-13.
- [9] Chadwick, S. G. and Haake, S. J., "The drag coefficient of tennis balls, The Engineering of Sport: Research, Development and Innovation, Blackwell Science, 2000, pp. 169-176.
- [10] Chadwick, S. G., "The Aerodynamics of Tennis Balls", PhD Thesis, University of Sheffield; 2003.